Contribution to inclusive (p, α) reactions from $(p, p\alpha)$ knockout at incident energies near 100 MeV

A. A. Cowley [*] and J. J. Van Zyl

Department of Physics, Stellenbosch University, Private Bag X1, Matieland 7602, South Africa

(Received 23 March 2021; accepted 24 June 2021; published 8 July 2021)

Background: The extent to which knockout, as opposed to a pickup reaction mechanism, contributes in pre-equilibrium (p, α) reactions is still not clear. Even with exclusive (p, α) reactions at conveniently low incident energies to well-defined final states, the issue often appears to be ambiguous. Recently Uozumi *et al.* [Y. Uozumi, Y. Fukuda, Y. Yamaguchi, G. Watanabe, and M. Nakano, Phys. Rev. C **102**, 014604 (2020)] used the intranuclear cascade (INC) theory to study pre-equilibrium (p, α) reactions in a range of incident energies from 42 to 300 MeV. They conclude that, below a projectile energy of about 120 MeV, knockout contributes almost nothing to the upper half of the pre-equilibrium (p, α) yield. This result is in disagreement with several other studies.

Purpose: We investigate whether existing $(p, p\alpha)$ quasifree knockout results support the conclusion from the INC study.

Method: The distorted-wave impulse approximation (DWIA) is used. The theory is known to give a good reproduction of experimental energy distributions and angular distributions, as well as absolute cross sections of $(p, p\alpha)$ reactions at incident energies at and above 100 MeV. The DWIA is simply exploited as a convenient way of interpolation and extrapolation of the available experimental distributions.

Results: The experimental cross-section distributions of the coincidence knockout reactions predict contributions to the pre-equilibrium yield much higher than those estimated by the INC study. At small scattering angles of only 30° to 40° the knockout yield is already quite substantial. At 60° it accounts for approximately all of the pre-equilibrium yield.

Conclusions: Even a lower-limit estimate of the coincident contribution at forward angles to the cross section of pre-equilibrium reactions is already sizable at low excitation. The cross section is expected to increase very rapidly at higher excitation energies (equivalently, lower α-particle energy).

DOI: 10.1103/PhysRevC.104.014608

I. INTRODUCTION

Recently Uozumi *et al.* [1] reminded us that, very surprisingly, in a (p, α) nuclear reaction the relative importance of knockout of a preformed α cluster in competition with pickup of three individual nucleons still needs to be satisfactorily resolved. Even where the transition proceeds to a well-defined final state in the residual nucleus, which greatly facilitates interpretation, results are often ambiguous. For pre-equilibrium reactions to excitations into the continuum the situation is even worse.

Of course, the fundamental reason for the difficulty is understood well. It originates from the property of direct transfer reactions [2] that their cross-section angular distributions are directly and profoundly influenced by the difference in momentum between the incident projectile and the emitted particle. All things considered, the difference of roughly a factor of 4 in mass between an incident proton and an outgoing α particle in a (p, a) transfer reaction already indicates the severity of the situation. In addition, this so-called momentum mismatch increases rapidly as a function of the incident energy for any specific nuclear reaction. Conservation of linear and angular momenta imposes a powerful constraint on the momenta of either picked-up nucleons or preformed clusters involved in a particle-transfer nuclear reaction. The momentum wave-function distribution of the nucleons and clusters bound in the target, and thus involved in the reaction, is normally not well known in the required range of momenta. Consequently this becomes a serious problem, especially at higher incident energy of interest to (p, a) pre-equilibrium reactions. The unfortunate outcome of this difficulty is that the cross-section prediction of, for example, the distorted-wave Born approximation theoretical formulation varies by orders of magnitude within the uncertainty of the bound-state momentum distribution towards higher momentum values.

The use of analyzing-power angular distributions, which are ratios of cross sections and consequently avoid the concern associated with absolute values, was postulated as a possible solution to the problem. This is an approach that we have pursued consistently in our recent studies [3–9] of pre-equilibrium reactions. Nevertheless, with the availability of an abundance of quantum-mechanical, classical, and phenomenological formulations [10] that address the same physics, it is essential to require consistency of conclusions from the various theoretical models.

Uozumi *et al.* [1] investigated the inclusive (p, α) reaction on a variety of target nuclei at incident energies between

*aac@sun.ac.za

42 and 300 MeV in terms of the intranuclear cascade (INC) model. They found that at proton incident energies at about 100 MeV and lower, knockout contributes practically nothing to the upper half of the α-particle spectrum. As Uozumi *et al.* [1] correctly point out, their prediction that knockout of preformed α clusters is negligible towards lower incident energies can be relatively easily checked against results from existing exclusive $(p, p\alpha)$ knockout reactions. However, as we show, this exercise is not as trivial as it intuitively appears.

In $(p, p\alpha)$ knockout reactions the flexibility of three-particle kinematics allows selection of experimental conditions under which the momentum of a struck (bound) α cluster remains fixed. Zero momentum of the α cluster, which corresponds to the so-called coplanar quasifree kinematic condition, is a popular option. Already many years ago, Roos *et al.* [11] demonstrated that the $(p, p\alpha)$ knockout reaction on targets up to ^{12}C is understood well enough to provide accurate spectroscopic factors. This translates directly into reliable cross-section reproductions by means of a distorted-wave impulse approximation (DWIA). This conclusion was confirmed later by Carey *et al.* [12] for a range of target nuclei up to ^{66}Zn.

The present work attempts to reconcile some of the conclusions of Uozumi *et al.* [1] with evidence based on published quasifree knockout investigations at comparable incident energy. For this we exploit the DWIA to provide guidance. We start from a kinematic region where experimental $(p, p\alpha)$ cross-section values for target nuclei in the desired mass range exist. We choose ^{58}Ni as a typical example comfortably close enough to the range of target species which Carey *et al.* [12] explored, and an incident energy of 100 MeV at which several $(p, p\alpha)$ investigations were performed. Then we use the DWIA to expand coverage of coordinate and momentum space for a reliable estimation of the resulting (p, α) yield associated directly with the knockout reaction.

Unfortunately our study suggests that Uozumi *et al.* [1] underestimate the contribution associated with knockout severely in the upper part of the continuum α-particle energy spectra at incident energies lower than about 120 MeV. The DWIA is a powerful and reliable tool for interpolation and extrapolation of the experimental $(p, p\alpha)$ data. It is reassuring that the quantitative information extracted is directly traceable to relevant measured knockout cross sections. This implies that the link between the experimental $(p, p\alpha)$ and (p, α) yields is highly likely to be an accurate assessment that is solidly based on two independent sets of measurements.

II. THEORETICAL DETAILS

A. Relationship between cross sections of (p, α) and $(p, p\alpha)$ reactions

To determine the contribution of the $(p, p\alpha)$ knockout yield to a pre-equilibrium reaction we simply integrate over the solid angle of the proton that is unobserved in the case of (p, α).

Because of the trivial relationship between $\frac{d^3\sigma}{d\Omega_p d\Omega_\alpha dE_p}$ and $\frac{d^3\sigma}{d\Omega_\alpha d\Omega_p dE_\alpha}$, depending on whether we need the notation to emphasize the fact that the same reaction may be equivalently written as either $(p, p\alpha)$ or $(p, \alpha p)$, we find

$$\frac{d^2\sigma}{d\Omega_\alpha dE_\alpha} = \int \frac{d^3\sigma}{d\Omega_\alpha d\Omega_p dE_\alpha} d\Omega_p. \tag{1}$$

However, the evident simplicity of the relationship between the (p, α) cross section and the coincident $(p, p\alpha)$ quantity obscures the complexity of the reaction process somewhat.

B. DWIA cross section

A brief description follows as a rough guide to the implications of the theoretical formulation of the DWIA. For convenience the notation of Chant and Roos [13] for a knockout reaction expressed as $A(a, cd)B$ is employed. Here $A = B + b$ and c is the quasifree-scattered projectile a after an interaction with the bound particle b, which is emitted from the target nucleus as particle d. In terms of the present $(p, \alpha p)$ reaction, this means that the incident particle $a = p$ and $c = \alpha$, with the emitted particle d identified with the unobserved proton in Eq. (1).

The differential cross section for such a reaction is expressed by Chant and Roos [13] as

$$\frac{d^3\sigma}{d\Omega_c d\Omega_d dE_c} = S_\alpha F_K \sum_{\rho_c' L\Lambda} \left| \sum_{\rho_a\sigma_a\sigma_c\sigma_c'} D^{s_a}_{\rho_a\rho_a'}(R_{ap}) \times D^{s_a^*}_{\sigma_c\sigma_c'}(R_{ac}) \times T^{L\Lambda}_{\sigma_a\sigma_c'\rho_a\rho_c'} \langle\sigma_c|t|\sigma_a\rangle \right|^2, \tag{2}$$

where S_α is a spectroscopic factor, F_K is a kinematic factor, the D_{mn} are rotation matrices which act on spin projections onto various axes as defined in Ref. [13]. For example, R_{ap} rotates the direction of propagation of the projectile a onto the polarization axis. The quantity $\langle\sigma_c|t|\sigma_a\rangle$ denotes the matrix element of the two-body p-α transition operator.

The quantity $T^{L\Lambda}_{\sigma_a\sigma_c'\rho_a\rho_c'}$ is expressed as

$$T^{L\Lambda}_{\sigma_a\sigma_c'\rho_a\rho_c'} = (2L+1)^{-1/2} \int \chi^{(-)*}_{\sigma_c'\rho_c'}(\mathbf{r})\chi^{(-)*}_{a}(\mathbf{r})\phi_{L\Lambda}(r) \times \chi^{(+)}_{\sigma_a'\rho_a}(\gamma\mathbf{r})d\mathbf{r}, \tag{3}$$

where $\gamma = A/B$, χ's represent the distorted waves for the incoming and outgoing particles, $\phi_{L\Lambda}$ is the bound-state wave function of the α cluster in the target nucleus, which represents the projection of the target wave function on the product of α-cluster and residual nucleus wave functions. A detailed description of the notation of Eq. (2) is provided in Refs. [13,14].

C. Factorization of the cross section

As is known [13,14], when spin-orbit terms are omitted in the distorting potentials for the protons (projectile and ejectile), the triple differential cross section reduces to the factorized form for the $(p, p\alpha)$ reaction:

$$\frac{d^3\sigma}{d\Omega_p d\Omega_\alpha dE_p} = S_\alpha F_K \left\{ \sum_\Lambda \left|T^{\alpha L\Lambda}_{BA}\right|^2 \right\} \left.\frac{d\sigma}{d\Omega}\right|_{p-\alpha}, \tag{4}$$

where $\frac{d\sigma}{d\Omega}|_{p-\alpha}$ is a half-shell two-body cross section for p-α scattering. The distorted momentum distribution for an α cluster in the target is the quantity $\sum_{\Lambda} |T_{BA}^{\alpha L\Lambda}|^2$.

In this work we exclusively use the unfactorized formalism for all calculations; therefore, it is not important whether factorization is a good approximation or not. However, it nevertheless serves as a guide to the general behavior of knockout cross-section distributions and their integrity over the available kinematic range of interest.

The extent to which factorization holds may be determined from experimental $(p, p\alpha)$ cross sections by taking into account quantities that remain approximately fixed by a proper choice of kinematic conditions. To be more specific, the cross-section data at specific angles and emission energies, such that zero recoil of the heavy residual nucleus is kinematically allowed, yields a quantity that is proportional to the two-body projectile-cluster cross section, as in the following expression:

$$\left.\frac{d\sigma}{d\Omega}\right|_{p-\alpha} = \left[\frac{d^3\sigma}{d\Omega_p d\Omega_\alpha dE_p}\right]_{\mathrm{EXP}} S_\alpha F_K \left\{\sum_{\Lambda} \left|T_{BA}^{\alpha L\Lambda}\right|^2\right\}, \quad (5)$$

where $[\frac{d^3\sigma}{d\Omega_p d\Omega_\alpha dE_p}]_{\mathrm{EXP}}$ now represents the experimental $(p, p\alpha)$ cross section.

Because the varying kinematic conditions are selected to keep the recoil momentum constant (usually at zero), the distorted momentum distribution $\sum_{\Lambda} |T_{BA}^{\alpha L\Lambda}|^2$ in Eq. (5) still remains roughly constant despite the angular variation of the two-body scattering. Roos *et al.* [11] discuss the reason for this in detail. In an explicit calculation they find a variation of less than 10% over the entire angular range of their experimental data. This is a typical result. Of course the spectroscopic factor S_α is a constant. Usually the kinematic factor F_K varies several orders of magnitude more slowly than the resultant extracted two-body cross section $\frac{d\sigma}{d\Omega}|_{p-\alpha}$.

Exploring the angular distribution of the quantity constructed with Eq. (5) in the center-of-mass of the colliding particles, and establishing how closely it follows free elastic scattering of protons from ^{4}He at the same incident energy, we are able to investigate to what extent the cluster reacts as a free entity to the interaction with the projectile.

Factorization tests of $(p, p\alpha)$ cross-section distributions have only been performed [11,15,16] on targets up to ^{12}C, but they are theoretically predicted [17] to hold even for very heavy nuclear targets.

D. Kinematic regions traditionally explored

Because of the considerable freedom of kinematic range in coordinate and momentum space offered by knockout reactions with three particles in the final state, it is usual to restrict investigations to a limited range.

Possible convenient choices are the following.

1. Quasifree two-body angular distribution

As was already partly discussed in Sec. II C, in this type of study the angles of observation of the two light emitted particles (p and α) are chosen to be quasifree coplanar sets in which the angular difference tracks the two-body half-shell p-α cross section in the center of mass. The values where the kinetic energies are of interest correspond to zero recoil momentum of the residual recoil heavy nucleus for knockout to the ground state. Through the impulse approximation this relates the recoil to zero momentum of the struck α cluster, hence linking the reaction process closely to free scattering [11,15,16].

2. Coplanar quasifree energy-sharing distribution

This type of arrangement explores the distribution of knockout yield along the kinematic locus corresponding to knockout to the ground state for a specific angle pair at which zero recoil momentum is kinematically allowed. The available total energy is shared by the emitted proton and α particle. From these distributions the distorted momentum distribution of a preformed α cluster in the target nucleus may be extracted.

Of course each angular set in the previous subsection may be exploited as a coplanar energy-sharing distribution.

3. Out-of-plane distribution

Only one investigation [18] of interest to us has been performed for this type of arrangement. Results confirmed expectation, with yield falling off smoothly with increasing angle out of the reaction plane as defined by the incident projectile and any one of the emitted light particles.

4. Angular correlations

An arrangement where the energy and the angle of the emitted α particle are held fixed as the secondary angle of the proton is varied would be most appropriate for reconstruction of a (p, α) cross-section angular distribution, but such configurations have not been studied in $(p, p\alpha)$ experiments. Fortunately, as will be shown, this information may be extrapolated with a reasonably high degree of confidence with guidance from the available energy-sharing and quasifree angular measurements.

As was mentioned in Sec. II C, all the angular correlations in this work are calculated with the complete unfactorized expression of Eq. (2). However, it may still be useful to keep the factorization approximation, expressed as Eq. (4), in mind if one wants to understand the features displayed in the plots of the theoretical angular correlations to be discussed later. In an angular correlation, the two crucial components of the factorized cross section are both simultaneously, yet differently, affected by the variation in recoil momentum. The same is true for the inevitable change in two-body kinematic conditions. This complicates interpretation of the detailed features of the calculated distributions somewhat.

III. CALCULATIONS

The contributions of α-cluster knockout to the ^{58}Ni(p, α) reaction at an incident energy of 100 MeV and an emitted α particle at an energy of 82 MeV at various forward-scattering angles were calculated in the DWIA. Our calculations rely on known global input quantities in an appropriate target mass range which is fairly wide; therefore, predicted cross-section

TABLE I. Optical model parameters. The factor ξ of the proton potentials, defined in Ref. [21], is close to unity. It converts the optical model potential strengths to the equivalent relativistic treatment used in the program THREEDEE.

	$p + ^{58}\mathrm{Ni} / p + ^{54}\mathrm{Fe}$, Ref. [21]	$\alpha + ^{54}\mathrm{Fe}$, Ref. [12]	$p + ^{4}\mathrm{He}$, Ref. [19]
V (MeV)	$\xi(117.5 - 14.34 \ln E_p - 50Z/A)$	161.77	$27.35 - 5.046 \ln E_p$
r_{0V} (fm)	1.21	1.26	1.577
a_{0V} (fm)	0.77	0.752	0.2
W (MeV)	7.4ξ	14.80	$6.55 + 0.06977E_p - 6.25 \times 10^{-5}E_p^2 + 2.321 \times 10^{-8}E_p^3$
r_{0W} (fm)	$1.37 + 3.5/A$	1.61	1.493
a_{0W} (fm)	$0.36 + 0.036A^{1/3}$	0.580	0.315
r_C (fm)	1.25	1.30	1.36
V_S (MeV)	$\xi(15 - 2.4 \ln E_p)$	—	$25.37 - 3.243 \ln E_p$
r_S (fm)	$0.985 + 0.0002A + 0.00064E_p$	—	0.879
a_S (fm)	$0.52 + 0.00086A$	—	0.303
W_S (MeV)	-1.2ξ	–	$5.69 - 1.355 \ln E_p$

results should be very similar for any target mass close to around 60 amu or so.

In using the DWIA for the extrapolation, care was taken to use distorting potential parameters, bound-state geometry parameters, and an on-shell approximation of the two-body cross section that are consistent with those in Refs. [11,12,16,18]. Those parameters are listed in Table I. From the work of Carey *et al.* [12], together with information from Refs. [11,16,18], this selection of input parameters ensures [12] that our predicted cross sections are reasonably reliable. Note that instead of using interpolated free elastic p-^{4}He cross sections, we use optical model potentials [19] to calculate cross sections in the effective incident energy range required for the integration procedure.

The choice of an outgoing α-particle energy of 82 MeV is governed by the need to remain in a range of excitation where the single-step intranuclear knockout is still likely to dominate. At much lower outgoing α-particle energy there is a higher probability that the knockout will be preceded by a nucleon-nucleon collision. The resulting reduced energy entering into the knockout process would unnecessarily complicate our simple estimation. The restriction to relatively small forward α-particle scattering angles originates from roughly the same consideration.

All calculations were performed with the code THREEDEE of Chant [20]. The spectroscopic factor S_α was set to unity, but this could be adjusted *post facto* if independent theoretical information for a specific target species justifies it.

IV. RESULTS AND DISCUSSION

Figure 1 shows angular correlations for the $^{58}\mathrm{Ni}(p, \alpha p)$ knockout reaction at an incident energy of 100 MeV. Various specific α-particle scattering angles θ_α as a function of the scattering angle θ_p of the proton in the reaction plane are shown. The reaction plane is defined by the incident beam and the direction of the α particle. The energy of the emitted α particle was chosen as 82 MeV, as motivated by the previous section.

Interpretation of the shapes of the knockout cross section as a function of the emitted proton angle, shown in Fig. 1, follows conveniently by keeping the factorized expression of Eq. (4) in mind. The principle was already outlined in Sec. II D 4.

Starting at small scattering angles θ_p, the two-body factor $\frac{d\sigma}{d\Omega}|_{p-\alpha}$ in Eq. (4), which behaves somewhat like free p-^{4}He elastic scattering, drops off more rapidly than the increase

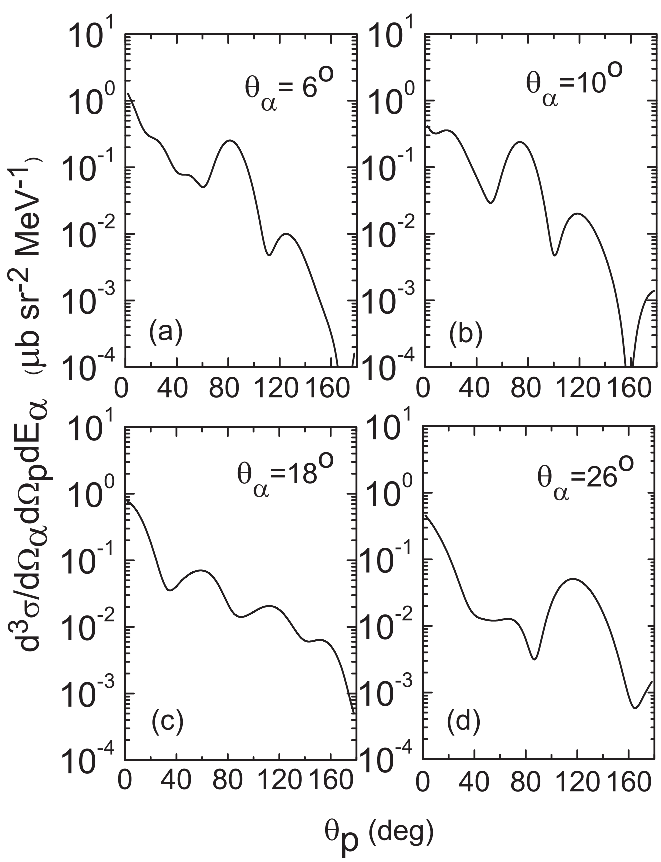

FIG. 1. DWIA angular correlations for the $^{58}\mathrm{Ni}(p, \alpha p)^{54}\mathrm{Fe(gs)}$ reaction at an incident energy of 100 MeV. Results are shown at the emission energy $E_\alpha = 82$ MeV and selected primary scattering angles θ_α as a function of the secondary angle θ_p.

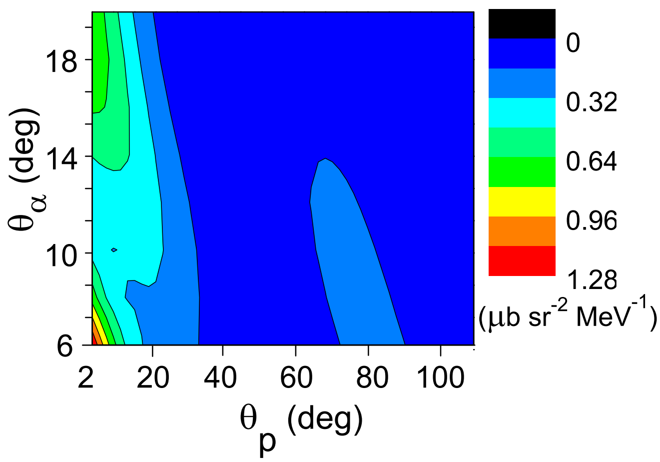

FIG. 2. Scatter plot of the distribution from which angular correlations of Fig. 1 were selected.

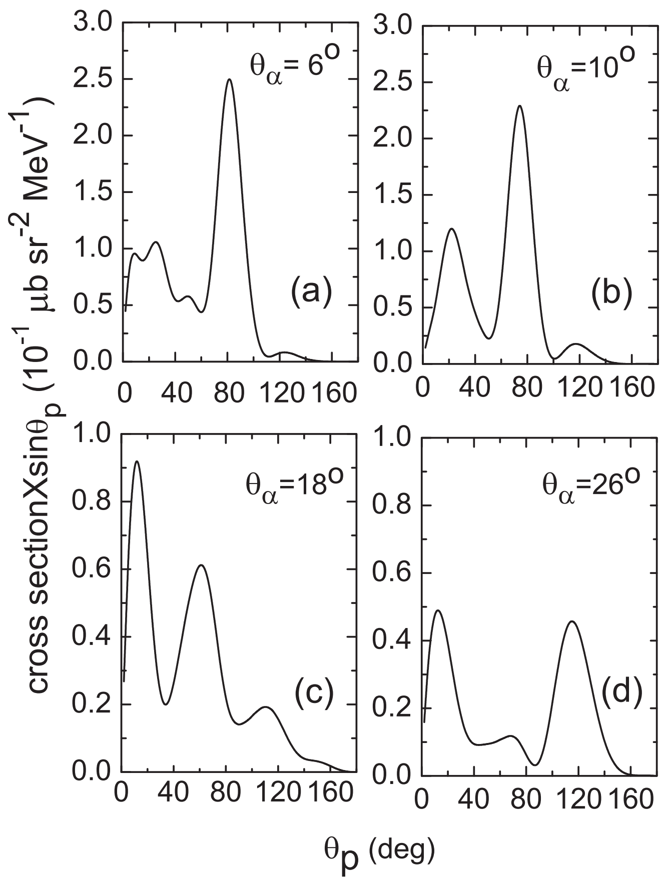

FIG. 3. Results of cross-section scales of Fig. 1 multiplied by sinθ_p to illustrate the distribution of relative weights to the integrated yield from the knockout reaction.

from the distorted momentum distribution compensates for. For small θ_α as in Fig. 1, the minimum recoil momentum allowed by kinematic constraints is eventually approached at some fairly large θ_p. Depending on how small the recoil momentum becomes, the more prominent the local cross-section increase resulting from the distorted momentum appears.

The overall result is an angular correlation that displays the two components of the factorized expression: a general drop-off of yield as a function of θ_p dominated by $\frac{d\sigma}{d\Omega}|_{p-\alpha}$, on which the response of the distorted momentum distribution is superimposed. However, one should keep in mind that the momentum distribution has smaller secondary maxima on either side of the main position, and these could also become prominent depending on kinematic conditions. In fact, we do observe evidence of exactly that.

In summary, the qualitative behavior of the angular correlations in Fig. 1 is understood well.

The absolute cross sections of Fig. 1 vary (in units of μb sr^{-2} MeV^{-1}) from 1 at the smallest proton angle θ_p to less than 10^{-4} at the largest scattering angle. Hence the trend is a general decrease from a maximum to a minimum, with some fluctuations in between. These absolute values may be compared with the range and trend of quasifree cross sections reported by Mabiala *et al.* [16] for ^{12}C$(p, p\alpha)^8$Be at the same incident energy. The cross sections in the present study are clearly systematically lower by about 2 orders of magnitude than the numerical experimental values listed in Ref. [16]. However, the variation between extreme cross-section values in the latter case is much smoother, as would be expected for a constant recoil momentum of zero. Of course, the cross sections of the present work are in reasonably good agreement with a simple rescaling of the values from Mabiala *et al.* [16] based on a larger recoil momentum, and if we also take the expected difference due to target-mass dependence [12] into account.

In Fig. 2 the results, which are partly shown in Fig. 1, are presented as a scatter plot. Note the presence of the peak associated with the distorted momentum distribution as it moves closer to quasifree scattering and the off-shell two-body interaction that is prominent towards forward proton
angles.

Figure 3 displays the same distributions as in Fig. 1, but it has the sinθ_p factor folded in to give better insight to the relative contribution to the in-plane integrated yield.

The estimation of yield from proton scattering angles β out of the reaction plane follows easily from our DWIA calculations if we exploit guidance from the work of Nadasen *et al.* [18] to simplify the integration process. As shown in Fig. 4, for ^{40}Ca$(p, p\alpha)$ the experimental cross section falls off approximately as a Gaussian distribution, as would be expected. As found by Nadasen *et al.* [18], the drop-off is the same irrespective of the outgoing proton energy E_p (or related E_α). This response is simply an artifact of the change in recoil momentum with angle β, which also affects the out-of-plane behavior at any proton angle θ_p in Figs. 1 and 3 in a similar way. Consequently the equivalent Gaussian trend holds for our DWIA calculations, except that the fall-off with out-of-plane angle β is found to be much wider, as anticipated for the different kinematic regions. Therefore a simple rescaling of the in-plane results should give a reasonably accurate approximation of the total integrated cross section. Whereas Fig. 4 predicts that about 25% of the cross section would be from

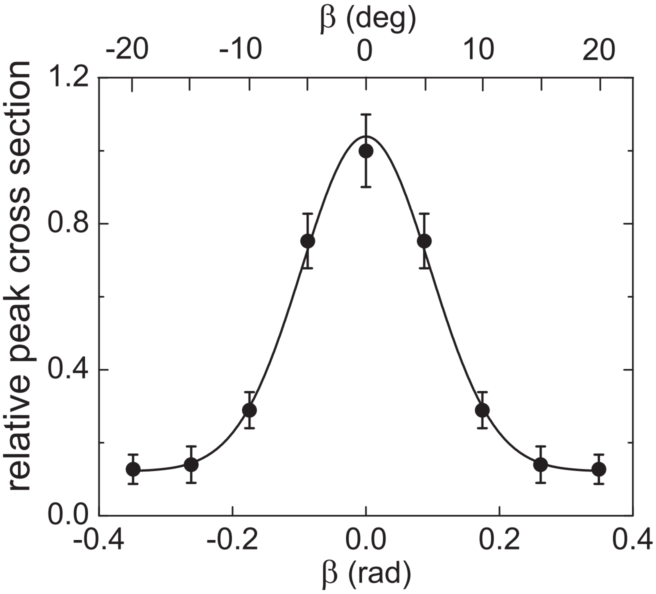

FIG. 4. Cross-section distribution out of the reaction plane defined by the incident beam and a primary angle. Data are from Nadasen *et al.* [18] at the peak of a quasifree energy-sharing distribution for the ^{40}Ca$(p, p\alpha)^{36}$Ar(gs) knockout reaction. A Gaussian distribution is used to estimate the contribution to the integrated yield. The same experimental data are plotted above and below the reaction plane as a reminder of the symmetry of the geometry.

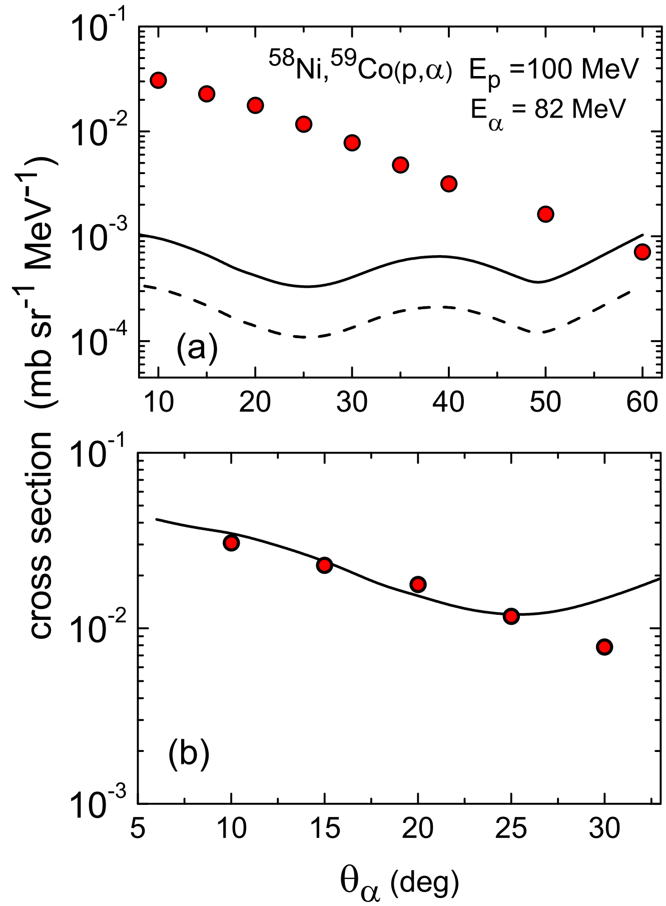

FIG. 5. DWIA prediction of the contribution from the ^{58}Ni$(p, \alpha p)^{54}$Fe(gs) knockout reaction at an incident energy of 100 MeV to the yield of an inclusive (p, α) reaction. An experimental cross-section angular distribution for the ^{59}Co(p, α) reaction [4] at the same incident energy is also shown as data points. (See text for reason and justification for using inclusive data from ^{59}Co(p, α) instead of ^{58}Ni). In panel (a) the dashed curve illustrates the result where the contribution from the knockout reaction would only be considered when both particles survive emission from the target system (in other words, the yield observed in a coincidence experiment). The solid curve in panel (a) shows the contribution to a (p, α) reaction where the α particle is observed irrespective of whether the unobserved proton suffers a further violent interaction with the residual nuclear system or not. In panel (b) the DWIA contribution is normalized to the experimental ^{59}Co(p, α) data to compare shapes of the angular distributions.

the out-of-plane yield, the wider distribution applicable to the kinematic range of interest to us predicts 50%.

Projected contributions to the inclusive ^{58}Ni(p, α) at an incident energy of 100 MeV originating from α-particle knockout in ^{58}Ni$(p, \alpha p)$ is displayed in Fig. 5(a). Appropriate experimental inclusive ^{58}Ni(p, α) data at the required incident and emission energy are not available. Fortunately, as Cowley [22] recently (re)confirmed, inclusive (p, α) cross-section energy and angular distributions are remarkably insensitive to the exact target species over a moderate range. Data for the target ^{59}Co is consequently expected to serve as an excellent substitute for ^{58}Ni(p, α). Everything else being the same, absolute cross-section values are confidently expected to disagree by not much more than overall experimental uncertainty.

If we require both emissions from the knockout reaction to emerge from the target system, we obtain the results shown as a dashed curve. This is a lower-limit result, because the emitted α particle from knockout will contribute to the (p, α) yield irrespective of whether the unobserved proton survives the interaction as a free particle. A simple, albeit realistic estimate of the alternative condition follows from treating the unobserved proton as a plane wave. The increased yield, estimated from a calculation at a representative quasifree position, is shown as the solid curve in Fig. 5(a). In Fig. 5(b) the shape of the knockout contribution is compared with that of the inclusive reaction.

In the INC analysis of Uozumi *et al.* [1], the contribution from knockout at comparable α-particle energy relative to the incident energy of 90 MeV in the ^{58}Ni(p, α) reaction does not even appear within 2 orders of magnitude lower, where their cross-section scale ends. The same is true for ^{59}Co(p, α) at an incident energy of 120 MeV in their work. Clearly the prediction of knockout yield from the DWIA treatment in our study considerably exceeds the expectation of the INC model analysis. Note that in Fig 5(a) the predicted knockout cross section at a scattering angle of 60° accounts for the total inclusive (p, α) yield. The clear inconsistency of the INC model with the results displayed in Fig. 5(a) needs to be explored more carefully in future studies.

It is interesting that the trend of the predicted angular distribution in Fig. 5(a) is in fairly good qualitative agreement with the knockout contribution at low excitation extracted by Dimitrova *et al.* [3] from a statistical multistep analysis for the reaction ^{90}Zr(p, α) at an incident energy of 72 MeV. Of course, the results from the latter study are driven by the need for good theoretical reproduction of the corresponding experimental analyzing power angular distribution. More information is needed to rule out fortuitous agreement.

V. SUMMARY AND CONCLUSIONS

We have investigated the contribution to inclusive (p, α) yield from a $(p, p\alpha)$ knockout reaction on a nuclear target mass in the range around 60 amu at an incident energy of 100 MeV. Existing experimental studies suggest that the reaction mechanism is understood well in terms of a DWIA formulation in the required mass and incident energy range. This provides trust for extrapolation and interpolation of yields, based on the DWIA theory, from experimental data. Furthermore, it is very unlikely that use of the DWIA could distort the estimation of the experimental integrated yield to an appreciable extent.

It is found that the knockout contribution to the inclusive (p, α) yield at high emission energy is considerably higher than anticipated by a recent INC study. Clearly expectations derived from the general behavior of $(p, p\alpha)$ knockout reactions suggest that the outcome of this investigation also holds for other target masses and at even lower incident energy.

The trend of $(p, p\alpha)$ knockout reactions towards much lower incident energy is often seriously misinterpreted simply because too much emphasis is placed on quenching of the distorted momentum distribution. One has to keep in mind that the two-body cross section increases much like elastic $p + {}^4$He scattering towards lower incident energy. The considerable simultaneous increase of sequential α-particle emission then obscures and complicates interpretation. It needs to be recalled that the knockout contribution to (p, α) comes from $(p, p\alpha)$ at low proton (high α) emission energy, whereas competing sequential processes originate from the opposite condition (high proton; low α energy). Whereas one process implicates positive α-cluster momentum, the other is associated with negative momentum. This simplifies studies such as the present one enormously.

Clearly the issues addressed here need to be clarified further. Additional studies would be highly desirable.

[1] Y. Uozumi, Y. Fukuda, Y. Yamaguchi, G. Watanabe, and M. Nakano, Phys. Rev. C **102**, 014604 (2020).

[2] G. R. Satchler, Rev. Mod. Phys. **50**, 1 (1978).

[3] S. S. Dimitrova, A. A. Cowley, E. V. Zemlyanaya, and K. V. Lukyanov, Int. J. Mod. Phys. E **27**, 1850091 (2018).

[4] A. A. Cowley, S. S. Dimitrova, E. V. Zemlyanaya, K. V. Lukyanov, and J. J. van Zyl, Phys. Rev. C **93**, 034624 (2016).

[5] S. S. Dimitrova, A. A. Cowley, E. V. Zemlyanaya, and K. V. Lukyanov, Phys. Rev. C **90**, 054604 (2014).

[6] S. S. Dimitrova, A. A. Cowley, J. J. van Zyl, E. V. Zemlyanaya, and K. V. Lukyanov, Phys. Rev. C **89**, 034616 (2014).

[7] A. A. Cowley, J. J. van Zyl, S. S. Dimitrova, E. V. Zemlyanaya, and K. V. Lukyanov, Phys. Rev. C **85**, 054622 (2012).

[8] A. A. Cowley, J. Bezuidenhout, S. S. Dimitrova, P. E. Hodgson, S. V. Förtsch, G. C. Hillhouse, N. M. Jacobs, R. Neveling, F. D. Smit, J. A. Stander, G. F. Steyn, and J. J. van Zyl, Phys. Rev. C **75**, 054617 (2007).

[9] A. A. Cowley, G. F. Steyn, S. S. Dimitrova, P. E. Hodgson, G. J. Arendse, S. V. Förtsch, G. C. Hillhouse, J. J. Lawrie, R. Neveling, W. A. Richter, J. A. Stander, and S. M. Wyngaardt, Phys. Rev. C **62**, 064605 (2000).

[10] P. E. Hodgson and E. Bêták, Phys. Rep. **374**, 1 (2003).

[11] P. G. Roos, N. S. Chant, A. A. Cowley, D. A. Goldberg, H. D. Holmgren, and R. Woody, Phys. Rev. C **15**, 69 (1977).

[12] T. A. Carey, P. G. Roos, N. S. Chant, A. Nadasen, and H. L. Chen, Phys. Rev. C **29**, 1273 (1984).

[13] N. S. Chant and P. G. Roos, Phys. Rev. C **27**, 1060 (1983).

[14] N. S. Chant and P. G. Roos, Phys. Rev. C **15**, 57 (1977).

[15] C. W. Wang, P. G. Roos, N. S. Chant, G. Ciangaru, F. Khazaie, D. J. Mack, A. Nadasen, S. J. Mills, R. E. Warner, E. Norbeck, F. D. Becchetti, J. W. Janecke, and P. M. Lister, Phys. Rev. C **31**, 1662 (1985).

[16] J. Mabiala, A. A. Cowley, S. V. Förtsch, E. Z. Buthelezi, R. Neveling, F. D. Smit, G. F. Steyn, and J. J. Van Zyl, Phys. Rev. C **79**, 054612 (2009).

[17] K. Yoshida, K. Minomo, and K. Ogata, Phys. Rev. C **94**, 044604 (2016).

[18] A. Nadasen, P. G. Roos, N. S. Chant, A. A. Cowley, C. Samanta, and J. Wesick, Phys. Rev. C **23**, 2353 (1981).

[19] W. T. H. van Oers, B. T. Murdoch, B. K. S. Koene, D. K. Hasell, R. Abegg, D. J. Margaziotis, M. B. Epstein, G. A. Moss, L. G. Greeniaus, J. M. Greben, J. M. Cameron, J. G. Rogers, and A. W. Stetz, Phys. Rev. C **25**, 390 (1982).

[20] N. S. Chant, Program THREEDEE (unpublished).

[21] A. Nadsasen, Ph.D. thesis, Indiana University, 1977; A. Nadasen, P. Schwandt, P. P. Singh, W. W. Jacobs, A. D. Bacher, P. T. Debevec, M. D. Kaitchuck, and J. T. Meek, Phys. Rev. C **23**, 1023 (1981).

[22] A. A. Cowley, Nucl. Instrum. Methods Phys. Res., Sect. A **977**, 164298 (2020).